Driving frequency effects on the mode transition in capacitively coupled argon discharges*

Liu Xiang-Mei(刘相梅), Song Yuan-Hong(宋远红)†, and Wang You-Nian(王友年)

School of Physics and Optoelectronic Technology, Dalian University of Technology, Dalian 116024, *China*

(Received 30 November 2010; revised manuscript received 30 January 2011)

A one-dimensional fluid model is employed to investigate the discharge sustaining mechanisms in the capacitively coupled argon plasmas, by modulating the driving frequency in the range of 40 kHz–60 MHz. The model incorporates the density and flux balance of electron and ion, electron energy balance, as well as Poisson's equation. In our simulation, the discharge experiences mode transition as the driving frequency increases, from the γ regime in which the discharge is maintained by the secondary electrons emitted from the electrodes under ion bombardment, to the α regime in which sheath oscillation is responsible for most of the electron heating in the discharge sustaining. The electron density and electron temperature at the centre of the discharge, as well as the ion flux on the electrode are figured out as a function of the driving frequency, to confirm the two regimes and transition between them. The effects of gas pressure, secondary electron emission coefficient and applied voltage on the discharge are also discussed.

Keywords: capacitively coupled plasma, mode transition, Ar discharge

PACS: 52.65.–y, 52.25.–b, 52.80.Pi **DOI:** 10.1088/1674-1056/20/6/065205

1. Introduction

Capacitively coupled plasma has been widely used for etching, deposition and other surface treatments in microcircuit manufacturing and material processing.[1−7] In the plasma enhanced chemical vapor deposition (PECVD), good understanding of the discharge properties, in particular the discharge mode, will assist in controlling and improving the film quality. Thus, various discharge modes and transitions between them have attracted much attention in recent years. Based on a theoretical model and some experimental results, Godyak *et al.*[8] showed the occurrence of an abrupt transition (from α mode to γ mode) in helium radio frequency (RF) discharge for moderate discharge pressures, as the RF voltage increased from 100 V to 2 kV. The transition into γ mode is accompanied by a sudden increase in the plasma density and decrease in the electron temperature of the bulk plasma. Also in this work, the theoretical model described satisfactorily the experiments in some cases, though a number of simplifying assumptions were adopted. To give a clear qualitative and quantitative description of this transition, a self-consistent fluid model was developed by Belenguer and Boeuf to analyse the existence of two different regimes.[9] The numerical results were in good agreement with the experimental measurements in Ref. [8] and the transition was attributed to a change from self-sustaining to power deposition heating. Other types of discharge transitions were also reported. For example, the transition from stochastic to collisional electron heating with increasing gas pressure,[10] and the transition from collisional to collisionless property (not stochastic heating) of the low-energy electrons as the low-frequency current increases, calculated by a particle-in-cell (PIC) simulation method with a Monte Carlo collision model (MCC).[11] Moreover, You *et al.*[12] studied the power dissipation mode transition, from ion-dominated to electron-dominated power dissipation, in a capacitively coupled plasma under the transverse magnetic field effect, with the comparison of experimental and theoretical results. More recently, a dissociative δ-mode being intermediate between α- and γ-modes was introduced in experimental studies on RF capacitive discharge in low-pressure NF_3, SiH_4,[13] and SF_6.[14]

However, despite the widespread investigations on mode transitions, the details of driving frequency effects on RF discharge in capacitively coupled plasma

*Project supported by the National Natural Science Foundation of China (Grant No. 10775025), the Scientific Research Fund of Liaoning Provincial Education Department for Colleges and Universities (Grant No. 2008T229), and the Program for New Century Excellent Talents in University (Grant No. NCET-08-0073).

†Corresponding author. E-mail: songyh@dlut.edu.cn

© 2011 Chinese Physical Society and IOP Publishing Ltd

are not yet well understood. Several recent publications have dealt with this issue,[15,16] but mainly focus on the characteristics of atmospheric pressure discharge with relatively larger frequencies ($\geq$ 2 MHz). Actually, the low radio-frequency plasma, in which ions have the possibility of obtaining higher energy within a long discharge cycle,[17,18] has also attracted much attention and already applied in the deposition of high-quality hydrogenated amorphous carbon (a-C:H) films and hydrogenated silicon nitride (SiN_x:H) films on Si and glass substrates.[19−21] Therefore, a wide range of the driving frequency, from 40 kHz to 60 MHz, is adopted in this work to focus on the basic discharge properties and mode transition in capacitively coupled plasma.

In this paper, based on a one-dimensional fluid model, the capacitively coupled Ar discharge for different driving frequencies is studied. The characteristics of plasma density, ion flux and electron temperature are of particular interest, since better understanding of them can assist in the design and optimization of the equipment and the discharge processes, as well as improving the deposition rate and the film growth in PECVD. Moreover, the effects of gas pressure, secondary electron emission coefficient and applied voltage on plasma properties are taken into account. The outline of this article is as follows: in Section 2 the theoretical model is described in detail, whereas the simulation results of the discharge mode transition are presented in Section 3. Conclusions are presented in Section 4.

2. Theoretical model

In this work, the RF source is applied to the lower electrode at $x = 0$ with the voltage waveform of $V(x = 0, t) = V_{\rm f} \sin(2\pi f t)$ and the upper electrode located at $x = L$ is grounded. No external blocking capacitors are considered because the discharge is symmetric between two planar electrodes with infinite radius. As the gas pressure here is set higher than or equal to 500 mTorr (1 Torr=1.33322 $\times$ 10^2 Pa), with the assumption of the discharge in local regime, a one-dimensional fluid model extended from that in Refs. [22] and [23] is adopted.

The fluid model includes the continuity equation, momentum balance, electron energy balance coupled with Poisson's equation, allowing self-consistent calculation of the electric field, particle densities and fluxes. The continuity equations for electrons and positive ions (Ar^+) are

$$\begin{aligned} \frac{\partial n_{\rm e}}{\partial t} + \frac{\partial \Gamma_{\rm e}}{\partial x} &= k_i N_b n_{\rm e}, \\ \frac{\partial n_i}{\partial t} + \frac{\partial (n_i u_i)}{\partial x} &= k_i N_b n_{\rm e}, \end{aligned} \tag{1}$$

where the electron flux $\Gamma_{\rm e}$ is estimated by drift-diffusion approximation and can be described by

$$\Gamma_{\rm e} = -\mu_{\rm e} n_{\rm e} E - \frac{D_{\rm e}}{T_{\rm e}} \frac{\partial (n_{\rm e} T_{\rm e})}{\partial x}, \tag{2}$$

and $n_{\rm i}$, $n_{\rm e}$ and $N_{\rm b}$ are the ion, electron and neutral gas densities. Moreover, the electron diffusion coefficient $D_{\rm e}$, mobility $\mu_{\rm e}$ and ionization coefficient $k_{\rm i}$ employed in the model are given in Refs. [23] and [24]. Owing to bigger ion mass compared with that of electrons, the momentum equation is introduced to calculate the ion velocity instead of the drift-diffusion approximation,

$$\frac{\partial u_{\rm i}}{\partial t} + u_{\rm i} \frac{\partial u_{\rm i}}{\partial x} = \frac{eE}{m_{\rm i}} - \nu_{\rm in} u_{\rm i}, \tag{3}$$

where $u_{\rm i}$ and $m_{\rm i}$ are the ion velocity and mass, respectively; $\nu_{\rm in}$ is the ion collision frequency with neutrals. As cold ion fluid model is adopted here, the pressure gradient term is not taken into account in Eq. (3). The electric field E and the potential V are calculated self-consistently from the Poisson's equation,

$$\frac{\partial^2 V}{\partial x^2} = -\frac{e}{\varepsilon_0} (n_{\rm i} - n_{\rm e}), \; E = -\frac{\partial V}{\partial x}, \tag{4}$$

where e is the elementary charge and ε_0 the permittivity of free space. Finally, the electron energy balance is introduced to investigate the electron temperature $T_{\rm e}$

$$\frac{\partial}{\partial t}\left(\frac{3}{2} n_{\rm e} T_{\rm e}\right) + \frac{\partial q_{\rm e}}{\partial x} = -e\Gamma_{\rm e} E - W_{\rm e}, \tag{5}$$

and the total electron energy flux $q_{\rm e}$ is given by

$$q_{\rm e} = \frac{5}{2} T_{\rm e} \Gamma_{\rm e} - \frac{5}{2} D_{\rm e} n_{\rm e} \frac{\partial T_{\rm e}}{\partial x}. \tag{6}$$

The energy loss due to inelastic collisions of electrons with neutrals can be given by $W_{\rm e} = \varepsilon_{\rm r} k_{\rm i} N_{\rm b} n_{\rm e}$, where $\varepsilon_{\rm r}$ = 15.6 eV is the ionization energy for Ar atoms. Here, there is no energy balance for ions with the assumption of local gas temperature. Since the neutral gas density $N_{\rm b}$ is much larger than the electron and ion density, we assume the neutral gas is uniformly distributed in the discharge room and $N_{\rm b}$ can be calculated by the ideal gas state equation

$$P = N_{\rm b} k_{\rm B} T_{\rm gas}, \tag{7}$$

where P is the gas pressure, $k_{\rm B}$ the Boltzmann constant and $T_{\rm gas}$ the neutral gas temperature.

The boundary conditions used in the fluid model are similar to those in Refs. [25] and [26]. The electron flux at the electrodes is given by $\Gamma_{\rm e} = \frac{1}{4}\upsilon_{\rm th} n_{\rm e}(1-\Theta) - \gamma_{\rm se}\Gamma_+$, where the interaction between electrons and the wall is taken into account, with the electron reflection coefficient $\Theta = 0.25$, the average electron thermal velocity $\upsilon_{\rm th} = \sqrt{8T_{\rm e}/\pi M_{\rm e}}$ and the positive ion flux $\Gamma_+ = n_{\rm i}u_{\rm i}$, $\gamma_{\rm se}$ is the secondary electron emission coefficient. The electron energy flux at the electrodes is defined as $q_{\rm e} = \frac{5}{2}T_{\rm e}\Gamma_{\rm e}$. Moreover, the ion flux and density at the electrodes are continuous, $\partial n_{\rm i}/\partial x = 0$, $\partial u_{\rm i}/\partial x = 0$.

3. Results and discussion

In this section, the calculation results are presented by using the one-dimensional fluid model, mainly discussing the influences of the gas pressure, the secondary electron emission coefficients and the applied voltage on the plasma discharge properties. We first set the gas pressure at $P = 0.5$ Torr, the RF voltage $V_{\rm f} = 300$ V and the secondary electron emission coefficient $\gamma_{\rm se} = 0.1$. A wide range of the driving frequencies from 40 kHz to 60 MHz is adopted in this simulation. The gas temperature and electrode spacing are kept as $T_{\rm gas} = 400$ K and $L = 3.0$ cm. Moreover, 100 grid points are employed in the axis direction, while the time-step Δt is set at 2.0×10^{-12} s. The discussion given below is based on the convergence of the fluid model, which ensures that the relative changes of the discharge parameters between two succeeding RF cycles are less than 10^{-6}.

Figure 1 shows the frequency variation profiles of the electron densities, with the gas pressure P set at 0.5 Torr, 1.0 Torr, and 2.0 Torr. The plasma densities given in the plot refer to those at the centre of the discharge, where the density profiles attain local maxima. It is clearly shown that there is a minimum point for the electron density at the frequency of 4 MHz, independent of the gas pressure. When the driving frequency $f < 4$ MHz (low frequency, LF region), the electron density decreases definitely with the increasing frequency. But as the frequency value $f > 4$ MHz (high frequency, HF region), increasing the driving frequency can lead to the increase of the electron density.

We can also find similar profile transitions at 4 MHz in Figs. 2 and 4, in which the frequency variation profiles of the ion flux on the electrode and the electron temperature at the centre of the discharge, are displayed, with the same discharge pressure values as those in Fig. 1. It is clearly seen in Fig. 2 that, the ion flux first decreases with the frequency and reaches a minimum value around the driving frequency of 4 MHz, resulting from the sheath edge shrinking with the frequency increasing and less ion energy obtained during the flight time in the sheath. The sheath shrinking with the frequency can be obtained from Fig. 3, in which the sheath thickness $D_{\rm sh}$ variation with the driving frequency is shown, with the sheath boundary defined as suggested by Economou *et al.*[27] And then, with the continuous increasing of the frequency after 4 MHz, the ion flux goes up slowly owing to the plasma density rises. And in Fig. 4, as the frequency increases, the electron temperature at the centre of the discharge experiences a sharp rise in the LF region and then keeps increasing but more gently as the driving frequency $f > 4$ MHz.

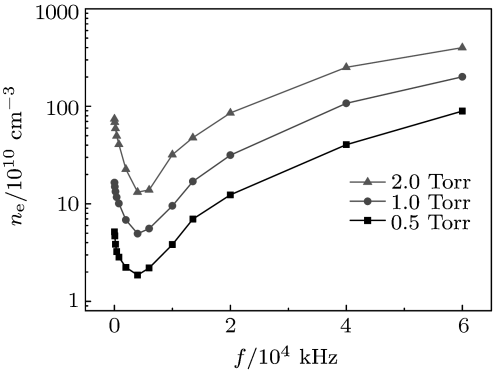


Fig. 1. Variation of the calculated electron density at the centre of the discharge as a function of the driving frequency at different gas pressures, as $P = 0.5$ Torr, 1.0 Torr, and 2.0 Torr, with $V_{\rm f} = 300$ V, $T_{\rm gas} = 400$ K, and $\gamma_{\rm se} = 0.1$.

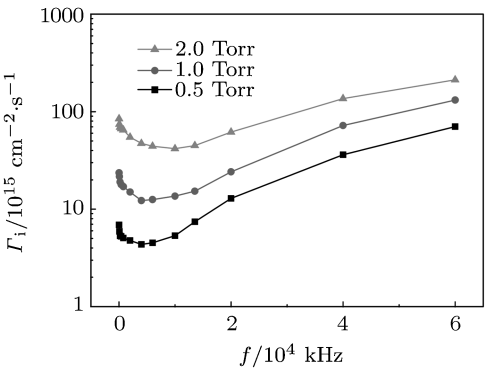


Fig. 2. Variation of the ion flux on the electrode as a function of the driving frequency at different gas pressures, with the same parameters settings as those in Fig. 1.

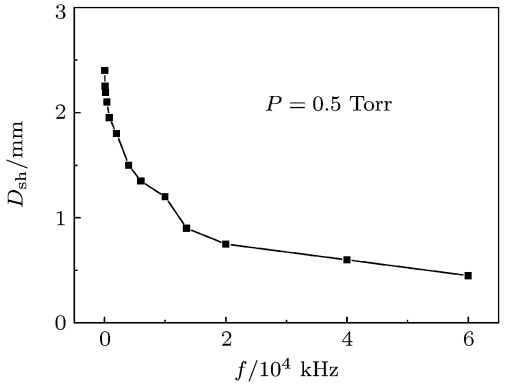


Fig. 3. Sheath thickness versus driving frequency at $P = 0.5$ Torr, with $V_f = 300$ V, $T_{gas} = 400$ K, and $\gamma_{se} = 0.1$.

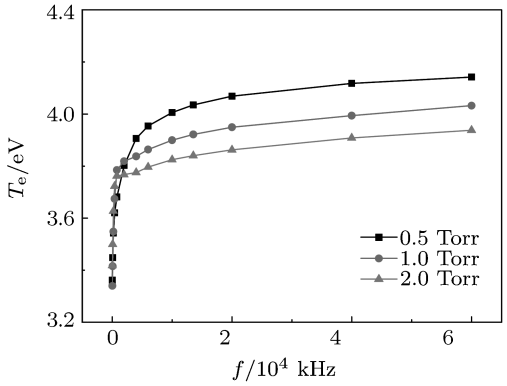


Fig. 4. Variation of the electron temperature at the centre of the discharge as a function of the driving frequency at different gas pressures, with the same parameter settings as those in Fig. 1.

The only reason for such a phenomenon is a mode transition arising around the driving frequency $f = 4$ MHz. In our opinion, at the LF region, due to higher ion energy on the electrode, more secondary electrons are definitely emitted from the electrodes under the ion bombardment and mainly responsible for self-sustaining discharge, which has been qualified as the γ mode. The lower the frequency, the thicker the sheath, as shown in Fig. 3 and hence a higher plasma density will be obtained. However, as the driving frequency increases continuously, particularly at the HF region, the secondaries do produce some ionization, but not enough, compared with the effect from the electron impact ionization. The collisions between electrons and neutrals play a major role in sustaining the plasma at this region. Thus, with the increase of the driving frequency and RF power, the plasma density keeps growing, showing properties of the α mode, in which the plasma density is proportional to the square of the driving frequency. So, in our calculation in which the driving frequency is concerned (from 40 kHz to 60 MHz), the discharge experiences a transition from γ to α mode. This simulation result is in good agreement with the experimental results,[4,8] in which it was found that the transition from α to γ mode is accompanied by a sharp drop in the electron temperature T_e and a sharp rise in the plasma density n_e.

It has also been noticed that the density profiles in Fig. 1 greatly depend on the gas pressure, in both LF and HF regions. Since more collisions between electrons and neutrals take place, the plasma densities become greater as the gas pressure increases. Similar calculation results can be obtained in Ref. [28], in which the influence of metastable atoms on the characteristics of capacitively-coupled Ar plasmas is mainly discussed. Due to the fact of the ion density, the ion flux in Fig. 2 increases sharply with the increase of gas pressure, particularly in the LF region, about one order of magnitude. On the other hand, because of the collision effect, electrons lose more energy with the increase of gas pressure at the HF region characterized as the α mode discharge, as shown in Fig. 4. However, at the LF region referred to as the γ mode, in which the electrons gain energy from secondary electron emission and sheath transport, rather than collisions, the electron energy shows less sensitive to the gas pressure.

In order to confirm the above discussion, the effect of the value of the secondary emission coefficient γ_{se} is studied in Figs. 5(a) and 5(b), in which the frequency variation profiles of the electron densities are shown, with the secondary electron emission coefficient γ_{se} set at five different values, while the gas pressure and the voltage are fixed. We can see from Fig. 5(a) that the electron density increases definitely with the increasing of secondary electron emission coefficient, in the LF region and near the transition point. Few increases can be observed in the HF region, particularly when the frequency is higher than 13.56 MHz. Thus, we can conclude that the discharge surely experiences a mode transition with the increasing of the driving frequency as we have discussed. Moreover, the frequency value corresponding to the transition point moves to a higher frequency region with the increase of the secondary electron emission coefficient. This result suggests the truth to us that more electrons emitted from the electrodes can take responsibilities for discharge maintenance compared with the electron impact ionization and delay the discharge mode transition from γ to α. We can also study the transition process much

clearly from Fig. 5(b), in which the driving frequency region we focus is reduced to that from 40 kHz to 6 MHz. In particular, it is noticed from this figure that, when the secondary electron emission coefficient is set at zero, the plasma density falls sharply to zero and the discharge cannot be sustained without the secondary electron emission, as the frequency is less than 2 MHz.

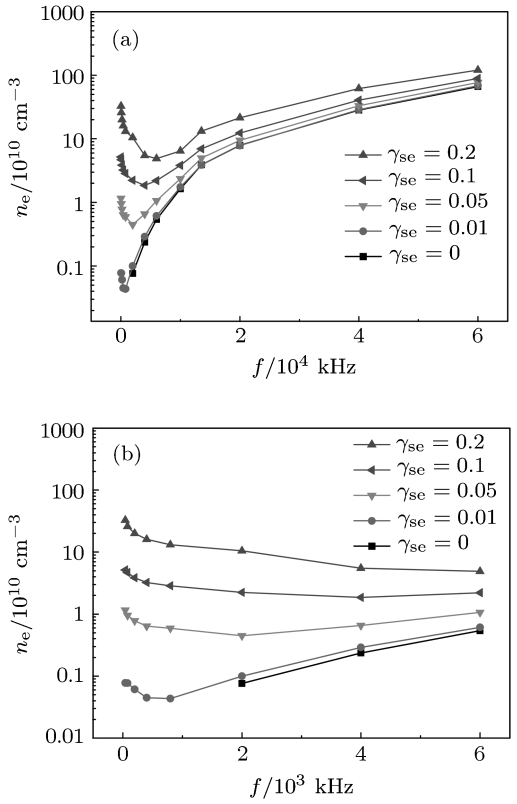


Fig. 5. Variation of the calculated electron density at the centre of the discharge as a function of the driving frequency, for different secondary electron emission coefficients, as $\gamma_{se} = 0$, 0.01, 0.05, 0.1, and 0.2, with $P = 0.5$ Torr, $V_f = 300$ V, and $T_{gas} = 400$ K, particularly for different regions of driving frequencies: (a) 40 kHz–60 MHz and (b) 40 kHz–6 MHz.

In Fig. 6, the frequency variation profiles of the electron densities at the centre of the plasma are shown, with the applied voltage V_f set at 300 V, 500 V, and 600 V. It can be noticed that the plasma density and the ion flux at the electrode increase definitely with the increasing of the applied voltage, as shown in Figs. 6 and 7, respectively. It is also observed in Fig. 7 that the transition frequency which corresponds to the minimum value of ion flux moves to higher frequency region with the increasing of applied voltage. This can be explained by the fact that, as increasing the voltage, the effect of the secondary electron heating can be enhanced. Note that, in the LF region, the electron density increases more distinctly with the increasing of applied voltage, suggesting us that the applied voltage has much greater impact on the secondary electron sustaining. Hence, with low frequencies drived in the discharge, the electron energy is more sensitive to the

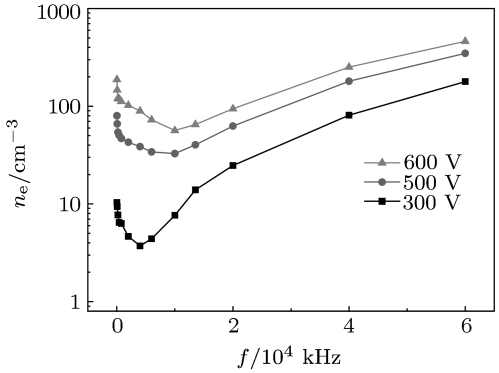


Fig. 6. Variation of the calculated electron density at the centre of the discharge as a function of the driving frequency, for different voltages, as $V_f = 300$ V, 500 V, and 600 V, with $P = 0.5$ Torr, $T_{gas} = 400$ K, and $\gamma_{se} = 0.1$.

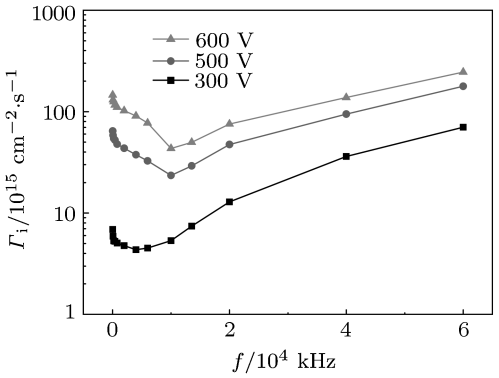


Fig. 7. Variation of the ion flux on the electrode as a function of the driving frequency, for different voltages, with the same parameter settings as those in Fig. 6.

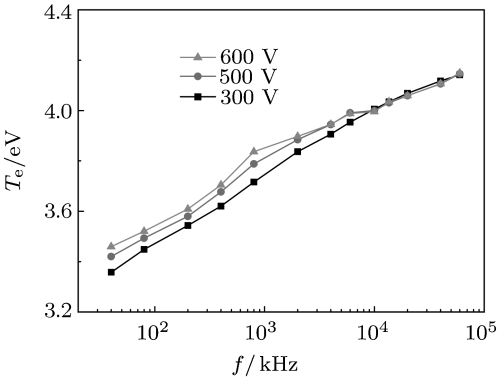


Fig. 8. Variation of the electron temperature at the centre of the discharge as a function of the driving frequency for different voltages, with the same parameter settings as those in Fig. 6. Note that the driving frequency is plotted on logarithmic coordinates.

increasing of the applied voltage than that in the HF region, as shown in Fig. 8, in which the driving frequency is plotted on logarithmic coordinates.

4. Concluding remarks

In summary, by using a self-consistent one-dimensional fluid model, we have studied the role of the driving frequency on the discharge regimes in the capacitively coupled argon plasmas. The simulation results show a mode transition from secondary electron heating to electron collision heating as the driving frequency increases from 40 kHz to 60 MHz. The effects of the gas pressure, secondary electron emission coefficient and applied voltage on the plasma density, ion flux and electron temperature are also discussed.

As the simulation results showed, the self-sustaining and power-deposition mechanisms are quite different for thr LF and HF region, which can be characterized as two regimes. In the LF region, characterized as the γ mode, the electron density declines rapidly accompanied by a sharp rise in the electron temperature as the frequency increases, suggesting less secondary electrons emitted from the electrode due to the decrease of sheath thickness and potential drop. On the other hand, in the high frequency region, defined as the α mode, the plasma density increases relatively slowly with the RF frequency, in agreement with the Townsend discharge property. In particular, without secondary electron emission, the discharge cannot even sustain in the frequency range of 40 kHz and 2 MHz. In the future work, we will extend our model to the case of two-dimensional fluid model and consider more about the detailed discharge process with different discharge parameters.

References

[1] Chapman B 1980 *Glow Discharge Process* (New York: Wiley) Chap. 5

[2] Berezhnoi S V, Kaganovich I K and Tsendin L D 1998 *Plasma Phys. Rep.* **24** 556

[3] Turner M M, Hutchinson D A W, Doyle R A and Hopkins M B 1996 *Phys. Rev. Lett.* **76** 2069

[4] Godyak V A, Piejak R B and Alexandrovich B M 1992 *Phys. Rev. Lett.* **68** 40

[5] Beneking C 1990 *J. Appl. Phys.* **68** 4461

[6] Godyak V A, Piejak R B and Alexandrovich B M 1991 *IEEE Trans. Plasma Sci.* **19** 660

[7] Yuan Y, Ye C, Huang H W, Shi G F and Ning Z Y 2010 *Chin. Phys.* B **19** 065205

[8] Godyak V A and Kanneh A S 1986 *IEEE Trans. Plasma Sci.* **PS-14** 112

[9] Belenguer Ph and Boeuf J P 1990 *Phys. Rev.* A **41** 4447

[10] Godyak V A and Piejak R B 1990 *Phys. Rev. Lett.* **65** 996

[11] Kim H C and Lee J K 2004 *Phys. Rev. Lett.* **93** 085003

[12] You S J, Chung C W, Bai K H and Chang H Y 2002 *Appl. Phys. Lett.* **81** 2529

[13] Lisovskiy V, Booth J P, Landry K, Douai D, Cassagne V and Yegorenkov V 2007 *J. Phys.* D: *Appl. Phys.* **40** 6631

[14] Lisovskiy V, Booth J P, Jolly J, Martins S, Landry K, Douai D, Cassagn V and Yegorenkov V 2007 *J. Phys.* D: *Appl. Phys.* **40** 6989

[15] Walsh J L, Zhang Y T, Iza F and Konga M G 2008 *Appl. Phys. Lett.* **93** 221505

[16] Moon Se Youn, Kim D B, Gweon B and Choe W 2008 *Appl. Phys. Lett.* **93** 221506

[17] Ni T L, Ke B, Zhu X D, Arefi-Khonsari F and Pulpytel J 2008 *Plasma Sources Sci. Technol.* **17** 045006

[18] Conti S, Porshnev P I, Fridman A, Kennedy L A, Grace J M, Sieber K D, Freeman D R and Robinson K S 2001 *Experimental Thermal and Fluid Science* **24** 79

[19] Shimozuma M, Tochitani G, Ohno H, Tagashira H and Nakahara J 1989 *J. Appl. Phys.* **66** 447

[20] Kang S S, Kim B S, Park D K and Yang S H 1996 *Phys. Rev.* B **54** 8919

[21] Lelievre J F, De la Torre J, Kaminski A, Bremond G, Lemiti M, Bouayadi Rechid El, Araujo Daniel, Epicier Thierry, Monna R, Pirot M, Ribeyron P J and Jaussaud C 2006 *Thin Solid Films* **511–512** 103

[22] Gogolides E and Sawin H H 1992 *J. Appl. Phys.* **72** 3971

[23] Bukowski J D, Graves D B and Vitello P 1996 *J. Appl. Phys.* **80** 2614

[24] Lymberopoulos D P and Economou D J 1993 *J. Appl. Phys.* **73** 3668

[25] Nitschke T E and Graves D B 1994 *J. Appl. Phys.* **76** 5646

[26] Boeuf J P and Pitchford L C 1995 *Phys. Rev.* E **51** 1376

[27] Economou D J, Evans D R and Alkire R C 1988 *J. Electrochem. Soc.* **135** 756

[28] Zhang Y R, Xu X and Wang Y N 2010 *Phys. Plasmas* **17** 033507